An In-Situ Observational Study on the Turbulent Characteristics in the Near-surface Layer during the Landfalling Period of Super Typhoon Maria (2018)

Chen Chen[1]

Jie Tang[1*] and Gerard Kilroy[2]

XiPing Zhang[1]and Li-min Lin[1],

Bing-ke Zhao[1], and Shuai Zhang[1]

[1] CMA Shanghai Typhoon Institute, Shanghai, China

[2] Meteorological Institute, Ludwig-Maximilians University of Munich, Germany

Submitted to GRL

[*]Corresponding author: Dr. Jie Tang (tangj@typhoon.org.cn)

Shanghai Typhoon Institute, China Meteorological Administration, Shanghai, China.

Key Points:

- The ocean-atmosphere drag coefficient during typhoon landfall is investigated for 10-min average wind speeds extend to 42.27 m s^{-1}.
- The relationship between the drag coefficient and wind speed is parabolic during typhoon landfall.
- The drag coefficient extreme drifting as height was mainly caused by the trends of the negative tangential turbulent fluxes with wind speed.

Abstract

The air-sea exchanges of momentum which are often parameterized by the variation of drag coefficient (C_{D}) and wind speed (u_{n}), is largely uncertain at typhoon-force extreme values of u_{n}. This paper investigated the relationship between C_{D} and extreme values of u_{n} for five different heights using the eddy covariance method from two coastal observation towers during the landfall of Super Typhoon Maria. In particular, our observations include 10-min average u_{n} extended to high wind speed of 42.27 m s^{-1}. The relationship between C_{D} and u_{n} was parabolic from regression analysis, and the "roll-off" of C_{D} and u_{*} appeared at about 28 m s^{-1}. From the bottom to top heights, the corresponding u_{n} of C_{D} extreme were 9.95, 12.72, 22.32, 32.57 and 38.04 m s^{-1}, respectively. The trend of negative tangential turbulent flux with u_{n} was found to be the main cause for the C_{D} extreme drifting with heights.

Plain Language Summary

The air-sea interaction is critical to the intensification of tropical cyclone because of the exchange of the momentum, humidity and energy between the atmosphere

and the ocean. The exchanges of momentum, which is the most important physical process, is often parameterized by the variation of drag coefficient and wind speed in numerical models, but the magnitude of the corresponding wind speed dependent drag coefficient is largely uncertain at typhoon-force extreme winds. This study investigated the variability of drag coefficient with wind speed at five different heights observations in a more extreme winds (> 35 m/s) during Super Typhoon Maria, results yield that the relationship between drag coefficient and wind speed was parabolic by regression analysis and the maximum of drag coefficient appeared at 30 m height rather than 10 m height using extensively in numerical models. It is the first observation study that revealed that the drag coefficient extreme drifting with height, and the trend of negative tangential turbulent flux with wind speed in onshore direction contributes mainly to the phenomenon. This finding may indicate a new way to improve air-sea interaction in boundary layer scheme of tropical cyclone and thus improve the intensity forecast.

1 Introduction

Air-Sea/land exchanges of momentum play an essential role in determining the interaction between the atmosphere and the underlying surface under the bulk transfer relationships based on the Monin-Obukhov similarity theory (MOST) (Monin and Obukhov, 1954) in the sea or land surface processes in weather and climate numerical models and applications in environment sciences and other geoscience (Wyngaard, 2010; Xiao et al., 2013; Zhu et al., 2013). The accuracy of the momentum flux parameter is depended on the drag coefficient (C_{D}) (or the bulk transfer coefficient over land, Nystrom et al., 2020). Over the past few decades, a number of observational and numerical experiments have been conducted to improve understanding of the sea/land-atmosphere exchange processes (Nolan et al., 2009; Zachry et al., 2013; Smith et al., 2017; Yu et al., 2020). These Include the Qinghai-Xizhang Plateau Meteorological Experiment (QXPMEX) in arid/semi-arid areas (Zhao et al., 2017), the Coupled Boundary Layer and Air-Sea Transfer Experiment (CBLAST) in the Atlantic (Black et al., 2007; French et al., 2007), the NOAA Hurricane Forecast Improvement Program and the Intensity Forecasting Experiment (IFEX-HFIP) (Rogers et al., 2012), and other experiments in the Western Pacific (Tang et al., 2015; 2018). Both theoretical work and field observations have investigated the relationship between C_{D} and wind speed (u_{n}) in different surface conditions. For extreme wind speeds (35 m s^{-1}), the trends of C_{D} and u_{n} are unclear with three different outcomes reported (increase, decrease and constant with changing u_{10}) in both observations and laboratory experiments (Alamaro et al., 2012; Cione et al., 2020).

The boundary layer of the eyewall region in tropical cyclones (TCBL) often has extremely wind speeds (Emanuel 1986; Kepert 2001). Previous studies point out that the mean C_{D} increases approximately linearly with increasing u_{n} at low and moderate wind speed in typhoons/hurricanes, but the divergence of the C_{D} trend appears during very strong winds. Furthermore, saturation points of

C_D differ from different observations on account of the impact of sea spray and waves and the critical wind speeds at which C_D levels off are between 15 to 40 m s^{-1} (Holthuijsen et al., 2012; Potter et al., 2014; Ming et al., 2015; Zhang et al., 2015; Duan et al., 2017; Hsu et al., 2019; Gao et al., 2020; Liu et al., 2020). For the open ocean, Powell et al. (2003, 2008) started to estimate C_D in tropical cyclones (TCs) by analyzed 2664 global positioning system (GPS) dropsondes and found that C_D reaches its maximum at wind speeds of about 33 m s^{-1} (near hurricane-scale strength). Moreover, Richer et al. (2021) used the flux-profile method to improve the result of Powell et al. (2003) and refreshed that the C_D versus u_{10} relationship does not actually exhibit a inflection point. Zhao et al. (2020) and Sparks et al. (2019) extended the saturation of C_D out to 60 m s^{-1} via the direct aircraft measurements in Pacific typhoons. More recently, unmanned aircraft were used to measure momentum fluxes near the eyewall of TCs with extremely high winds up to 87 m s^{-1} (Cione et al., 2020). Both of them found the uncertain of the measurements in high winds affect the relationship between C_D and u_n. From near shore the corresponding u_n of the C_D saturation seems lower than that in open ocean, Bi et al. (2015), Zhao et al., (2015) and Fang et al. (2018) showed that C_D leveled off when wind speeds around 18-24 m s^{-1} using the eddy covariance (EC) method, while the trend of C_D at winds beyond roughly 35 m s^{-1} is unavailable due to wave breaking and water depth. Hsu et al. (2019) noticed the sea surface wave and estimated its impact on C_D, and detected the indeterminacy when winds larger than 30 m s^{-1}. In laboratory, Troitskaya, et al. (2012, 2020) pointed out that C_D reaches a maximum at a little larger values of u_n around 25 m s^{-1} under small-scale surface waves conditions. By using a stepped frequency microwave radiometer (SFMR) measurements on the aircraft, Bell et al. (2012) pointed out that calculations were at least 50% more uncertain at higher wind speeds. To our best knowledge, insufficient experiments have documented the quantitative value of C_D in ultra-high wind conditions ($>$ 35 m s^{-1}), especially at height above 10 m nearshore. As a result, the relationship of high u_n and C_D at different heights in a typhoon-like circulation has been, until recently, poorly understood to verify turbulent flux parameterizations in TCs (Kepert 2012; Li & Pu, 2020).

Although ample evidence suggests C_D is affected by fetching, wave breaking, sea spray and foam (Zhao et al., 2015), Mostly C_D in models is calculated based on u_n only (Akbar et al. 2017). In order to determine C_D nearshore and provide a reference for the modeling community, the main objective of this study is thus to find the relationship between the C_D and u_n during observations of typhoon via five height levels data of EC measurements from two different EC flux towers (one tower is at the top of an island hill and the other one is nearshore), In particular, an aim is to determine C_D with extreme values of u_n from 10 m to 130 m heights during typhoon landfall. In section 2, the data and processing methods used are introduced. Section 3 presents the results of the data analysis. Section 4 includes a summary of the main findings and future work.

2 Data and analysis methods

2.1 Data overview

In this study, the data analyzed were collected from two onshore EC flux towers deployed along the coastline at Sansha, Fujian, China during the passage of Typhoon Maria (1808). The lower tower (26°55 30 N, 120° 13 46 E, 60 m above sea level (a.s.l)) was approximately 10 m from the coastline, as indicated in Figure 1a, and is referred to as the Low Tower in this study. The High Tower (26°55 25 N, 120°13 54 E, 120 m a.s.l.) was deployed at the top of the hill, as indicated in Figure 1b, and is referred to as the High Tower. The distance between the two towers is about 150 m. The underlying surface of the two towers is grass with less than 0.1 m height.

Four three-dimensional ultrasonic anemometers were mounted on the two towers with 1.5 m cantilever brackets at 10, 30, 50 and 70 m heights above the ground. The four three-dimensional ultrasonic anemometers (WindMaster^{TM} Pro 3D, Gill Instruments Limited) and a high-performance data logger with a sampling rate of 20 Hz (CR3000, Campbell Scientific Instruments Inc., Logan, UT, USA) were combined to make a flux measurement system. Unfortunately, the extreme gust wind speed observed is about 50.1 m s^{-1} during the landfall of Maria caused the collapse of the High Tower, thus measurements from the sonic anemometers were collected from four levels from the Low Tower nearshore in the period from 0000 local standard time (LST) July 10 to 0000 LST July 12 and a level of 50 m of the High Tower at the top of the hill before landfall (130 m above the nearshore ground and 170 m a.s.l.).

2.2 Review of Super Typhoon Maria

Super Typhoon Maria (2018) was the eighth typhoon to form in the Northwest Pacific Ocean in 2018. Figure 1 presents the track of Typhoon Maria relative to the location of the two EC flux towers, and shows also the intensity evolution using data from Shanghai Typhoon Institute of China Meteorological Administration (http://www.typhoon.org.cn/) (Ying et al., 2014). Maria made landfall over Lianjiang County of the Fujian Province in China at 0850 LST July 11 2018 which was approximately 68 km away from the two observation towers. The towers at this time were located in the inner core region of the circulation, with the radius of maximum wind (RMW) at this time being close to 60 km (Bao et al., 2020). A maximum 10-min average wind speed of 42.27 m s^{-1} was observed at 50 m height of the Higher observation Tower. After landfall Maria continued its track northward while weakening rapidly as a result of land effects.

2.3 Methodology introduction

In the EC method, a friction velocity (u_*) is defined as

(1)

where , and are wind fluctuations in the streamwise. The over bar expresses Reynolds averaging.

The C_{D} under the neutral stability condition is estimated by

(2)

where is the Reynolds-horizontal mean wind velocity at the observation heights z (Garratt, 1977), n is the height of measurements taken on the towers.

2.4 Data Processing and Quality Control

The original anemometer data pre-processing in this study mainly involves outlier removing, tilt correction, coordinate rotation corrections and linear detrending (Lee et al., 2004). Schmid et al. (2001) proposed a method to inspect the power spectra of turbulent fluctuations and we followed that method in this study.

(1) The spikes in the data sets were removed by using a criterion of X(h) < (X - 4) or X(h)> (X + 4), where X(h) denotes the original data, X is the mean over the averaging interval and is the standard deviation.

(2) The calculation of C_D were omitted when the corresponding u_* less than 0.01 m s^{-1}. No gap filling was token in this study.

(3) Based on the coastline features near the measurement site, we found that the offshore flow wind direction ranges from 52.5-227.5°, and the offshore flow ranged from 272.5° to 5°. The wind data (249-269°) from the back of the measurements from the Lower Tower and the wind data (68-88°) from the back of the measurements from Higher Tower were removed due to the turbulent eddies generated by the tower.

3 Results and discussions

3.1 The variation of C_D and u_* against u_n

Figure 2a-b provides the variation of C_D as a function of u_n derived from the five levels of the two towers during Typhoon Maria. Despite the large scattering of C_D, C_D at all levels showed a clear parabolic trend with u_n when regressed from the median values of C_D (Figure 2b). C_D had an increasing trend with an increase in u_n (1-28 m s^{-1}), and beyond this range, a saturation or a level off of was observed at higher u_n. The trends in C_D with increasing u_n was similar to the coastal wind measurements from Zachry et al., (2013). From the bottom to top heights, the corresponding u_n of C_D extreme were 9.95, 12.72, 22.32, 32.57 and 38.04 m s^{-1}, respectively.

Figure 2c-d depicts that the variations in u_* with u_n at different heights using the bin-averaged method. Like the trend of C_D with $u_{n,}$ the total u_* also increased with increasing u_n up to 28 m s^{-1}, and decreased for u_n above 28 m s^{-1}. The trends in u_n agrees reasonable well with previous studies that reported variation in u_* with u_n both over open ocean and coastal observations (Zhao et al., 2015; Fang et al., 2020). But the saturation of u_* at a faster wind speed than that from Fang et al. (2020), it may due to the nearer distance from the core of typhoon center.

3.3 Vertical profile of C_D and u_*

In order to investigate the structure of C_D and u_* with heights, the vertical profile of C_D and u_* with varying u_n for the sixteen hours during Maria landfall's period is analyzed in Figure 3a-b. As Typhoon Maria approached the coastline, the values of C_D increased rapidly from 02:00 to 07:00 LST 11 July, as the tower was located between 3 RMW and RMW from the typhoon center. It reached a maximum value of C_D at 30 m height (10.148) at 06:00 LST 11 July (Figure 3a). While the amplitude of C_D decreased noticeably when the towers were located in the eyewall region (< RMW) from 07:00 to 12:00 LST 11 July. After landfall, C_D increased again from 12:00 to 14:00 LST 11 July when the towers were located 3-5 RMW from the typhoon center, and the C_D of 30 m height became the largest of the different levels again. During these times the amplitude of C_D was much smaller than that during the pre-landfall period. It may be implied that the values of C_D before Typhoon Maria landfall were bigger than these after landfall, and the values of C_D from the 2-3 RMW were bigger than those in RMW. Similar to the discussions above, the vertical variation of u_* was highly consistent with C_D before the Maria landfall and u_* in the 2-3 RMW is bigger than that in RMW (Figure. 3b). That is to say, the momentum exchange flux was more severe in the 2-3 RMW is bigger than that in RMW. It was consistent with the expected behavior of these physical quantities in the typhoon boundary layer (Kepert 2001).

3.4 The variation of C_D and u_* with u_n at each height from regressed results

To understand further the details of the variations of C_D with u_n at different heights, regressed from the median and mean numbers were completed by generating groups at each height and are plotted against u_n in Figure 4a-e. According to the regression curves, the relationship between the median or mean values of C_D and wind speed were parabolic from 10 m to 70 m height, while C_D presented as a curve of two peaks from 130 m height. The first peak appeared in the wind speed section of 10-20 m s^{-1} under the offshore winds, the second peak arose at the wind speed section of 28-38 m s^{-1} under onshore winds.

From the bottom to top height, the C_D saturation points were 0.06, 0.05, 0.62, 0.17 and 0.01 from 10, 30, 50, 70, 130 m heights, respectively, and the corresponding wind speeds were about 18, 18, 23, 28 and 38 m s^{-1}.The saturation values of C_D decrease along with the increasing wind speeds from 30 m to 130 m height, it seems that the regression curves of the median and mean C_D had a drifting of saturation as height. The values of C_D reached their maximum with wind speeds of 18 m s^{-1} at 30 m height rather than 10 m height currently used in various surface flux parameterization of models. In other words, one might conclude that surface roughness had less impact on airflow when the height exceeds 30 m.

In a comparison of the saturation values of C_D from the Lower Tower at nearshore with those on the same height of the Higher Tower on the hilltop (50 m height), we see that the saturation C_D value at 50 m height from the Higher Tower was smaller than those from the same height at the Lower Tower from nearshore. According to Eq.2, u_n from the Higher Tower was higher than

that from the Lower Tower, while the u_* from the Higher Tower was lower than that from the Lower Tower. This could explain the lower C_{D} from the Higher Tower. This may imply although u_{n} increased with height, the momentum fluxes were not always similarly increasing with height, and the weaker influence of the ground and the higher wind speed led to a decreasing C_{D} with height. Topography may also affect the decrease rate of C_{D} with heights. The surface of the earth exerts a frictional drag on the air blowing just above it, the difference in terrain conditions directly affects how much friction is exerted. Hills affects the wind speed and/or change wind direction much more, so that the u_* values from the Higher Tower clearly decreased leading to decreasing $C_{\mathrm{D.}}$

Similar to the analysis of C_{D}, the variations of u_* with u_{n} at different heights calculating by the bin-averaged method are shown in Figure 4f-j. The median, mean and maximum u_* are also plotted in Figure 4f-j. From the bottom to top heights, the u_* saturation points were 2.74, 2.88, 5.453, 3.35 and 1.99 m s^{-1} at 10, 30, 50, 70, 130 m height, respectively, and the corresponding u_{n} were about 18, 23, 28, 33 and 38 m s^{-1} regressing from the mean and median u_* data. This finding indicates that the drifting in saturation of u_* was responsible for the drifting in saturation of C_{D} with height. The u_* maximum increased from 10 m to 50 m height, then it decreased at larger heights. The maximum u_* occurred at 50 m height with a value of 5.6134 m s^{-1}, which was higher than to the maximum of C_{D} appeared at 30 m height. The vertical variation trend of u_* is consistent with Fang et al. (2020), and it indicates that u_* does not always decrease with height under typhoon condition. However, French et al. (2007) reported that u_* has a decreasing trend with height above 70 m and below 400 m height under typhoon conditions. The different results obtained in this study from ground to 170 m height suggest that the boundary layer structure is complicated and it needs more observations of the u_* vertical profile to confirm.

From our dataset, the critical u_{n} located nearshore at 10 m height (20.5456 m s^{-1}) was similar to the leveling off point of 22 m s^{-1} from Fang et al. (2018), but it a little bit smaller than that of 26-30 m s^{-1} reported by Zhao et al. (2015). The differences in critical wind speed from the different sectors in TCBL and different underlying surfaces.

3.5 The variation of the turbulent flux ($\overline{w'u'}, \overline{w'v'}$) with u_{n} at each height

In order to explore which part of turbulent flux generates the drifting of saturation and extreme in C_D and u_* with height, Figure 5 presents scatters plot of positive turbulent fluxes ($\overline{w'u'}, \overline{w'v'}$) and negative turbulent fluxes ($-\overline{w'u'}$,$-\overline{w'v'}$) against u_{n} from the five heights. The trend of negative tangential component fluxes ($-\overline{w'u'}$) with u_{n} was agree well with the trend of u_* and C_{D} again u_{n}, rather than the trend of radial components flux ($\overline{w'v'}$) with u_{n}. The corresponding u_{n} with extreme $-\overline{w'u'}$ in each height were constant with extreme C_{D} highly. Furthermore, the extreme wind conditions ($>$ 35 m s^{-1}) in onshore direction concentrated at the negative component fluxes, it may be concluded that the variation of the $-\overline{w'u'}$ in onshore direction was the main factor of C_{D}

drifting with $u_{n.}$

4 Summary and Conclusion

In this study, high frequency wind data was collected by two EC flux towers located on the coastline of the East China Sea to study the turbulent characters and eddy transportation during the passage of Super Typhoon Maria. In contrast to most previous studies on turbulence in high wind speeds at low levels (<50 m a.s.l), this study investigates the values of the C_D from five height levels at two towers from the near surface (70, 90, 110, 130 and 170 m a.s.l). The extreme 10-min average u_n is 42.27 m s^{-1} and the minimum distance to the landing point of typhoon is less than 70 km which shows the relationship between C_D and u_n in a more extreme environment (> 35 m s^{-1}) in the upper surface layer (170 m a.s.l). Furthermore, comparing the near shore observational results with the hilltop observations at high winds, it is confirmed that the dependence of C_D on u_n is modified by elevation. Some preliminary conclusions are offered as follows.

According to regression from the median of total data, the relationship between C_D and u_n was parabolic, the "roll-off" of u_* also appeared at about 28 m s^{-1}. From the bottom to top heights, the corresponding u_n of C_D extreme were 9.95, 12.72, 22.32, 32.57 and 38.04 m s^{-1}, respectively. The C_D saturation points were 0.06, 0.05, 0.62, 0.17 and 0.01 at 10, 30, 50, 70, 130 m heights, respectively, and the corresponding wind speeds were 18, 18, 23, 32 and 38 m s^{-1}. For the first time observed, the saturation and extreme values of C_D had a drifting with heights based on in-situ observations. Moreover, the regression curve of the median and mean u_* also had a drifting of saturation u_* with height like C_D. Furthermore, the trends of the extreme negative tangential turbulence fluxes in onshore direction was the main cause for C_D extreme drifting with u_n.

It is worth noting that the maximum C_D appeared at 30 m height rather than 10 m height currently used in various surface flux parameterization of models. An obviously decreases in C_D in upper level (>30 m height) of the lower boundary layer was found. This may imply that due to the increasing height, there is a weaker influence from the ground. The values of C_D from the 2-3 RMW was bigger than that in RMW. These information would enhance our understanding of the turbulent process in the TCBL.

Observations in high winds are relatively rare, and more in-situ observations needed to confirm the drifting of extreme C_D in the future. In addition, further work will explore the enthalpy exchange coefficient from different sectors of typhoon/hurricane structure to update in the understanding of the air-sea drag under extreme wind conditions, and thus improve the turbulent process in the typhoon numerical models.

Acknowledgments

This study was supported jointly by the Key Program for International S&T Cooperation Projects of China (No.2017YFE0107700), National Key R&D Pro-

gram of China (No.2020YFE0201900) and the Research Program from Science Foundation of China (41475060 and 41775065). The study is also supported by the ESCAP/WMO Project (EXOTICCA), National Natural Science Foundation of China (No.42075056) and Shanghai S&T Research Program (No.19dz1200101).We thank the Editor, and anonymous reviewers for their helpful comments that greatly improved the original manuscript.

Data Availability Statement

The eddy covariance observation data in this paper are available online https://figshare.com/articles/dataset/EC_observation_data_during_Typhoon_Maria_rar/16566162 (DOI:10.6084/m9.figshare.16566162).

References

Alamaro, M., Emanuel, K. A., Colton, K. A., McGillis, W. R. & Edson, J.(2002). Experimental investigation of air-sea transfer of momentum and enthalpy at high wind speed. paper presented at 25th Conference on hurricanes and Tropical Meteorology, *American Meteorology Society*, San Diego, Calif., 29 Apr to 3 May (2002).

Al-Jiboori, M. H. (2010). Determining of neutral and unstable wind profiles over Baghdad city, *Iraqi Journal of Science, 51*, 343–350.

Bao, X., Wu, L., Zhang, S., Yuan, H., &Wang, H. (2020). A comparison of convective raindrop size distributionsin the eyewall and spiral rainbands of Typhoon Lekima (2019). *Geophysical Research Letters, 47*, e2020GL090729.https://doi.org/10.1029/2020GL090729

Bell, M. M.,Montgomery, M. T., & Emanuel, K. A. (2012). Air–sea enthalpy and momentum exchange at major hurricane wind speeds observed during CBLAST, *Journal of the Atmospheric Sciences, 69*, 3197–3222. doi: 10.1175/jas-d-11-0276.1

Black, P. G., Asaro E. A. D, Sanford, T. B., Drennan, W. M., Zhang, J. A., French, J. R., Nüler, P. P., Terrill,E. J. & Walsh, E. J. (2007). Air-sea exchange in hurricanes: Synthesis of observations from the Coupled Boundary Layer Air-Sea Transfer experiment, *Bulletin of the American Meteorological Society, 88*, 357–374. doi:http://dx.doi.org/10.1175/BAMS-88-3-357

Bi, X., Gao, Z., Liu, Y., Liu, F., Song, Q., Huang, J., Huang, H., Mao, W., & Liu, C. (2015). Observed drag coefficients in high winds in the near offshore of the South China Sea. *Journal of Geophysical Research: Atmospheres, 120*, 6444–6459.

Cione, J. J., Bryan, G. H., Dobosy, R., Zhang, J. A., De Boer, G., Aksoy, A., Wadler, J.B., Kalina, E. A., Dahl, B. A., Ryan, K., Neuhaus, J., Dumas, E., Marks, F. D., Farber, A. M. Hock, T., & Chen, X. (2020). Eye of the storm: observing hurricanes with a small unmanned aircraft system. *Bulletin of the American Meteorological Society, 101*, 187–205.

Curcic, M., & Haus, B. K. (2020). Revised estimates of ocean surface drag in strong winds. *Geophysical Research Letters*, *47*, e2020GL087 647, doi:10.1029/2020GL087647

Duan, Z., Yao, X., Li, Y., Lei, X., Fang, P., & Zhao, B. (2017). Investigation of turbulent momentum flux in the typhoon boundary layer. *Journal of Geophysical Research:Oceans, 122*, 2259–2268.

Emanuel, K. A. (1986). An air–sea interaction theory for tropical cyclones. Part I:Steady-state maintenance, *Journal of the Atmospheric Sciences, 43*,585–604.

Fang, P., Jiang, W., Tang, J., Lei, X., & Tan, J. (2020). Variations in Friction Velocity with Wind Speed and Height for Moderate-to-Strong Onshore Winds Based on Measurements from a Coastal Tower. *Journal of Applied Meteorology and Climatology,59*,637–650.

Fang, P., Zhao, B., Zeng, Z., Yu, H., Lei, X., & Tan, J. (2018). Effects of wind direction on variations in friction velocity with wind speed under conditions of strong onshore wind. *Journal of Geophysical Research: Atmospheres, 123*, 7340–7353.

French, J. R., Drennan,W. M., Zhang, J. A., & Black, P. G. (2007). Turbulent fluxes in the hurricane boundary layer, Part I: Momentum flux. *Journal of the Atmospheric Sciences, 64*,1089–1102. https://doi.org/10.1175/JAS3887.1

Garratt, J. R. (1977). Review of drag coefficients over oceans and continents, *Monthly Weather Review, 105*, 915–929. doi:10.1175/1520-0493(1977)105<0915:RODCOO>2.0.CO;2

Gao Z., Peng,W., Gao,C., & Li, Y. (2020). Parabolic dependence of the drag coefficient on wind speed from aircraft eddy-covariance measurements over the tropical Eastern Pacific. *Scientific Reports,10*,1805(2020).https://doi.org/10.1038/s41598-020-58699-9

Grachev, A. A., Fairall, C. W., & Larsen, S. E. (1998). On the determination of the neutral drag coefficient in the convective boundary layer, *Boundary-LayerMeteorology,86*,257–278, doi:10.102

3/A:1000617300732

Holthuijsen, L.H., Powell M.D. & Pietrzak, J.D. (2012). Wind and waves in extreme hurricanes. *Journal of Geophysical Research:Oceans, 117*,C09003. https://doi. org / 10.1029 /2012JC007983,

2012

Hsu, J.Y., Lien, R.C., D'Asaro, E. A., & Sanford, T. B. (2019). Scaling of drag coefficients under five tropical cyclones. *Geophysical Research Letters, 46*, 3349–3358, doi:10.1029/2018GL081574

Jarosz, E., Mitchell, D. A., Wang, D. W., & Teague, W. J. (2007). Bottom-up determination of air-sea momentum exchange under a major tropical cyclone.

Science, 315, 1707–1709. https://doi.org/10.1126/science.1136466.

Hsu, J.Y., Lien, R.C., D'Asaro, E. A., & Sanford, T. B. (2017). Estimates of Surface Wind Stress and Drag Coefficients in Typhoon Megi, *Journal of Physical Oceanography, 47*, 545–565. doi:10.1175/JPO-D-16-0069.1

Kepert, J. D. (2012). Choosing a boundary layer parameterization for tropical cyclone modeling. *Monthly Weather Review,140*, 1427–1445. https://doi.org/10.1175/MWR-D-11-00217.1

Kepert, J. D. (2001). The dynamics of boundary layer jets within the tropical cyclone core. Part I: Linear theory. *Journal of the Atmospheric Sciences, 58*, 2469–2484.

Lee, X., Yu,Q., Sun, X., Liu, J., Min, Q., Liu, Y., & Zhang, X. (2004). Micrometeorological fluxes under the influence of regional and local advection: a revisit. *Agricultural Forest Meteorology 122*,111–124.

Li L.,Xiao, Y., Zhou, H., Xing, F., & Song, L.(2018). Turbulent wind characteristics in typhoon Hagupit based on field measurements. *International Journal of Distributed Sensor Networks, 14*.https://doi.org/10.1177/1550147718805934

Li, X., & Pu, Z. (2020). Vertical eddy diffusivity parameterization based on a large-eddy simulation and its impact on prediction of hurricane landfall. *Geophysical Research Letters*, 48, e2020GL090703. https://doi.org/10.1029/2020GL090703

Liu, C, Li,Y., Gao, Z., Zhang, H., Wu, T., Lu, Y., & Zhang, X.(2020). Improvement of drag coefficient calculation under near-neutral conditions in light winds over land. *Journal of Geophysical Research:Atmospheres,125*,(24). https://doi.org/10.1029/2020JD033472

Ming, J., & Zhang, J. A. (2018). Direct measurements of momentum flux and dissipative heating in the surface layer of tropical cyclones during landfalls. *Journal of Geophysical Research: Atmospheres, 123*, 4926–4938. https://doi.org/10.1029/2017JD028076

Monin, A.S., & Obukhov, A.M. (1954). Basic laws of turbulent mixing in the surface layer of the atmosphere. *Contributions to Geophysics and Geodesy, USSR Academy of Sciences (151)*, 163–187.

Nolan, D. S., Zhang, J. A., & Stern, D. P. (2009). Evaluation of planetary boundary layer parameterizations in tropical cyclones by comparison of in-situ data and high-resolution simulations of Hurricane Isabel (2003). Part I: Initialization, maximum winds, and outer core boundary layer structure. *Monthly Weather Review,137*, 3651–3674. https://doi.org/10.1175/2009/

MWR2785.1

Nystrom, R. G., Chen, X., Zhang F., & Davis, C.A. (2020). Nonlinear Impacts of Surface Exchange Coefficient Uncertainty on Tropical Cyclone Intensity and Air-Sea Interactions. *Geophysical Research letter,47*,e2019GL085783.

Potter, H., Graber, H.C., Williams, N.J., CollinsI,C.O., Ramos, R. J., & Drennan, W.M. (2014). In situ Measurements of Momentum Fluxes in Typhoons. *Journal of the Atmospheric Sciences,72(1)*,104–118.

Powell, M. D. (2008). High wind drag coefficient and sea surface roughness in shallow water. *Final report to the Joint Hurricane Tested, April 2007*, 26 pp.

Powell, M. D., Vickery, P. J., & Reinhold, T. A. (2003). Reduced drag coefficient for high wind speeds in tropical cyclones. *Nature, 422*, 279–283.

Richter, D.H., Wainwright, C., Stern, D.P., Bryan, G.H., & Chavas., D. (2021). Potential low bias in high-wind drag coefficient inferred from dropsonde data in hurricanes. *Geophysical Research letter,47*. https://doi.org/10.1175/JAS-D-20-0390.1.

Rogers, R., Aberson, S., Aksoy,A., Annane,B., Black,M., & Cione, J., et al. (2013). NOAA's Hurricane Intensity Forecasting Experiment: A Progress Report, *Bulletin of the American Meteorological Society, (v.94)n.6,*859-882.

Schmid, H. P., Grimmond, C. S. B., Cropley, F., Offerle, B., & Su, H. B. (2000). Measurements of CO_2 and energy fluxes over a mixed hardwood forest in the mid-western United States, *Agriculture Forest Meteorology 103*,357–374, doi:http://dx.doi.org/10.1016/S0168-1923(00)0014-

4

Smith, R.K., Zhang, J.A., & Montgomery, M.T. (2017). The dynamics of intensification in a Hurricane Weather Research and forecasting simulation of Hurricane Earl (2010), *Quarterly Journal of The Royal Meteorological Society,143(702)*, 293–308.

Sparks, N., Hon, K. K., Chan, P. W., Wang, S., Chan, J. C. L., Lee, T. C., & Toumi, R. (2019). Aircraft observations of tropical cyclone boundary layer turbulence over the South China Sea. *Journal of the Atmospheric Sciences*, 76, 3773–3783, doi:10.1175/JAS-D-19-0128.1.

Tang, J., Zhang, J. A., Aberson, S. D., Marks, F. D., & Lei, X. (2018). Multilevel tower observations of vertical eddy diffusivity and mixing length in the tropical cyclone boundary layer during landfalls. *Journal of the Atmospheric Sciences,75(9)*, 3159-3168.

Tang, J., Byrne, D., Zhang, J. A., Wang, Y., Lei, X., Wu, D., Fang, P., & Zhao, B. (2015). Horizontal transition of turbulent cascade in the near-surface layer of tropical cyclones. *Journal of the Atmospheric Sciences, 72(12)*, 4915–4925.

Troitskaya, Y. I., Sergeev, D., Vdovin, M., Kandaurov, A., Ermakova,O., & Takagaki, N. (2020). A laboratory study of the effect of surface waves on heat and momentum transferat high wind speeds. *Journal of Geophysical Research: Oceans*, 125, e2020JC016 276, doi:10.1029/2020JC016276

Takagaki, N., Komori, S., Suzuki, N., Iwano, K., Kuramoto, T., Shimada, S., Kurose, R., & Takahashi, K. (2012). Strong correlation between the drag coeffi-

cient and the shape of the wind sea spectrum over a broad range of wind speeds, *Geophysical Research Letters, 39(23)*, L23604, doi:10.1029/2012GL053988

Wyngaard, J.C. (2010), Turbulence in the atmosphere. *Cambridge University Press*, New York.

Xiao, W., Liu, S., Wang, W., Yang, D., Xu, J., Cao, C., Li, H., & Li, X. (2013). Transfer coefficients of momentum, heat and water vapour in the atmospheric surface layer of a large freshwater lake. *Boundary Layer Meteorology 148*, 479–494. https://doi.org/10.1007/s10546-013-

9827-9

Ying, M., Zhang,W., Yu, H., Lu,X., Feng, J., Fan,Y., Zhu,Y., & Chen, D. (2014). An overview of the China Meteorological Administration tropical cyclone database. *Journal of Atmospheric and Oceanic Technology, 31(2)*, 287–301. doi: 10.1175/JTECH-D-12-00119.1

Yuan, J., Song, L., Chen, W., Zhi, S., Bi, X., liu, C., & Huang, H.(2020). Characteristics of Drag Coefficient in Different Coastal Regions of the South China Sea Under Tropical Cyclones-An Observational Study, *Journal of Tropical Meteorology,26(4)*,417–427.https://doi.org/10.46267/j.10

06-8775.2020.036

Yu, M., González,j., & Miao, S. (2020). Evaluation of a mechanical drag coefficient formulation in the complex urban area of Beijing, *Theoretical and Applied Climatology, 142(08)*, 743–749.

Zachry, B. C., Schroeder., J. L., Kennedy, A. B., & Hope, M. E. A. (2013). A case study of near shore drag coefficient behavior during Hurricane Ike, *Journal of Climate and Applied Meteorology, 52(9)*, 2139–2146, https://doi.org/10.1175/JAMC-D-12-0321.1 (2013).

Zhao, Z., Liu, C., Li, Q., Dai, G., Song, Q., & Lv, W. (2015). Typhoon air-sea drag coefficient in coastal regions. *Journal of Geophysical Research: Oceans, 120(2)*, 716–727.

Zhao, P., Xu, X., Chen, F., Guo, X., Zheng, X., Liu, L., Hong, Y., Li, Y., La, Z., Peng, H., Zhong, L., Ma, Y., Tang, S., Liu, Y., Liu, H., Li, Y., Zhang, Q., Hu, Z., Sun, J., Zhang, S., Dong, L., Zhang, H., Zhao, Y., Yan, X., Xiao, A., Wan, W., Liu, Y., Chen, J., Liu,G., Zhaxi, Y., & Zhou, X. (2017). The Third Atmospheric Scientific Experiment for AMERICAN METEOROLOGICAL SOCIETY Understanding the Earth-Atmosphere Coupled System over the Tibetan Plateau and Its Effects. *Bulletin American Geological Society, 99(4)*, 757–776. doi:10.1175/BAMS-D-16-0050.1

Zhao, Z., Chan, P.W., Wu, N., Zhang, J.A., & Hon, K.K. (2020). Aircraft observations of turbulence characteristics in the tropical cyclone boundary layer. *Boundary Layer Meteorology, 174*,493–511, doi:10.1007/s10546-019-00487-8.

Zhang J.A., & Marks, F.D. (2015). Effects of horizontal eddy diffusivity on tropical cyclone intensity change and structure in idealized three-dimensional numerical simulations. *Monthly Weather Review,143*(10), 3981–3995.

Zhu, P. & Furst, J. (2013). On the parameterization of surface momentum transport via drag coefficient in low-wind conditions, *Geophysical Research Letters,40*(11),2824–2828. doi:10.1002/ gr.0518

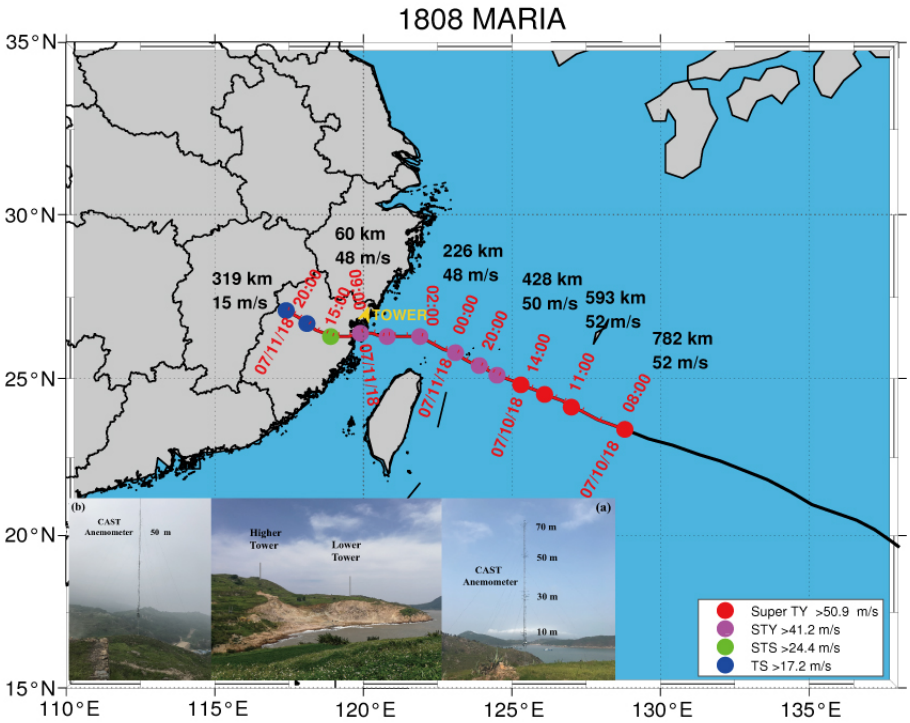

Figure 1 Track of typhoon Maria, the location, exposure and instruments of the two eddy covariance flux towers. The coastal observation towers are denoted by yellow arrow. (a) A photo of coastal observation tower approximately 10 m from the coastline, as indicated in Figure 1a, and is referred to as the Lower Tower in this study. The four levels of CAST anemometers on Lower Tower are 10 m, 30 m, 50 m and 70 m above the ground (70 m, 90 m, 110 m and 130 m a.s.l). (b) A photo of the coastal observation tower at the top of the hill, as indicated in Figure 1b, and is referred to as the Higher Tower in this study. The CAST anemometers on Higher Tower is 50 m above the ground (170 m a.s.l).

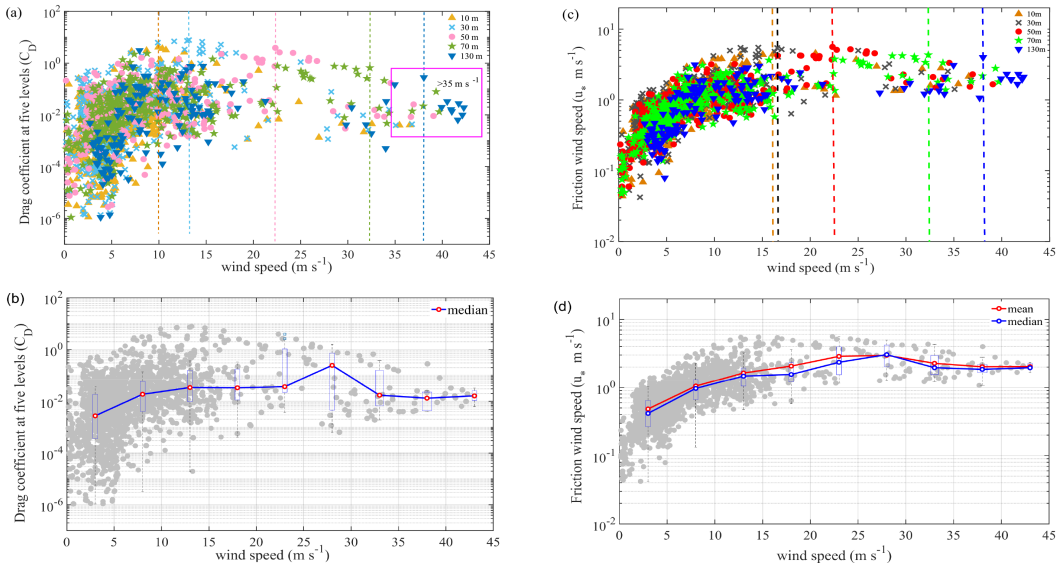

Figure 2 (a) Scatterplots of drag coefficient (C_D) versus wind speed (u_n) from the five levels during Typhoon Maria, as well as for the samples of 10 m (yellow triangles), 30 m (light blue crosses), 50 m (pink circles), 70 m (green star) and 130 m (blue circles). (b) Relationship of C_D versus u_n (gray dots), the blue line with red circle is the bin median averaged C_D with 5 m s^{-1} interval of u_n from observations. (c) Scatterplots of friction wind speed (u_*) versus u_n from the five levels during Typhoon Maria, as well as for the samples of 10 m (yellow triangles), 30 m (gray crosses), 50 m (red circles), 70 m (green star) and 130 m (pink circles). (d) Relationship of u_* with u_n (gray dots), the blue line with blue circles indicates the bin median averaged u_* with 5 m s^{-1} interval of u_n from observations, the red line with red circle represents the bin mean averaged u_* with 5 m s^{-1} interval of u_n from observations.

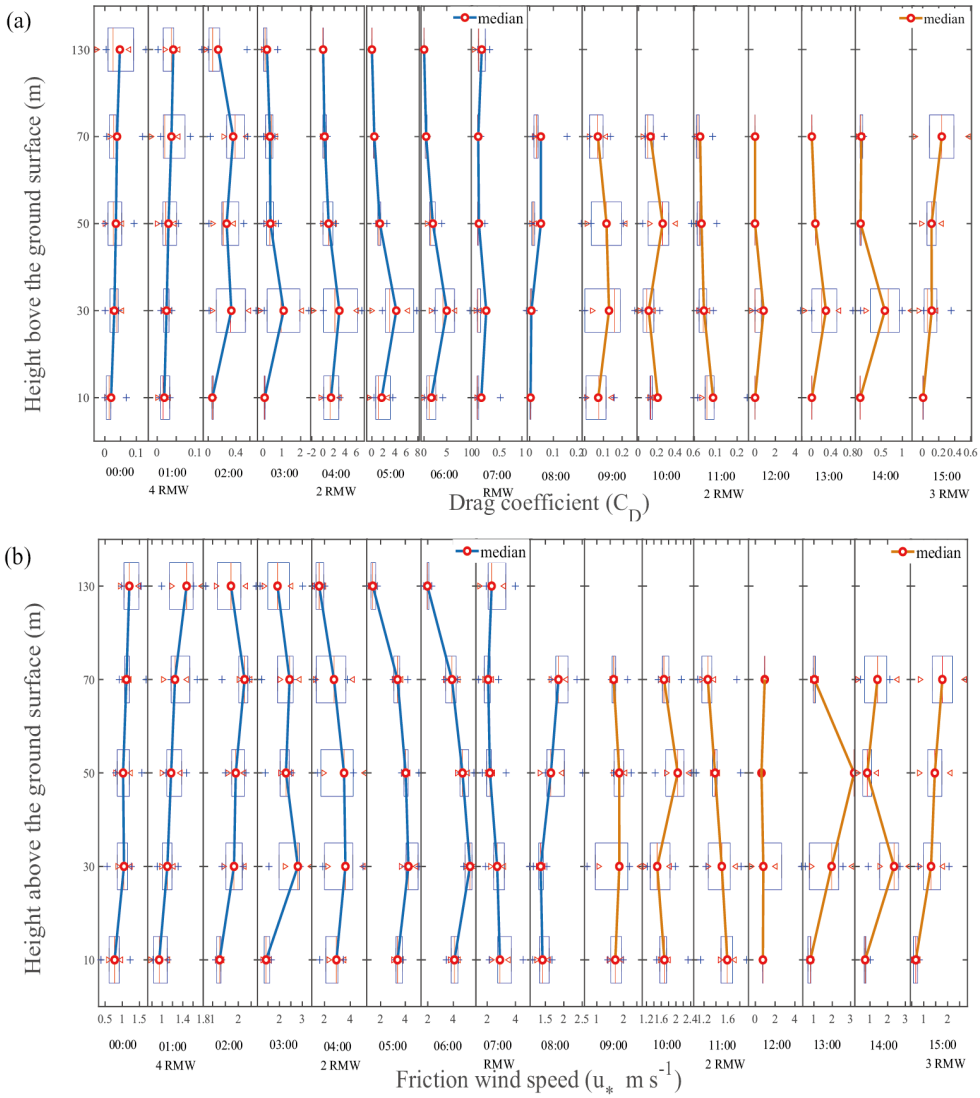

Figure 3 The vertical profile of (a) 10 min averaged drag coefficient (C_{D}) and (b) friction velocity (u_*), for sixteen hours before and for six hours after Maria landfall. The light blue line of (a) is the median of C_{D} at five heights. The blue line in (b) is the median of u_* at five heights. The left and right boundary lines are 25% and 75% percentage points.

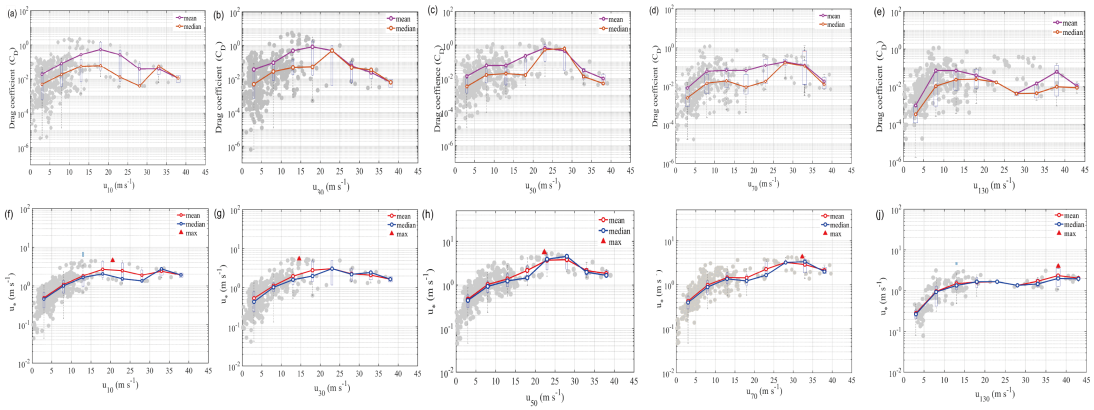

Figure 4 Variation in C_D (a-e) and u_* (f-j) with u_n at five different levels using the bin-averaged method from the two EC flux towers during Typhoon Maria. The purple and the orange lines in a-e are the regression line of mean and median C_D, respectively. The red and blue lines in f-j are the regression line of mean and median u_*, respectively. The red triangle in f-j are maximum of u_* in each groups (every 5 m s^{-1}).

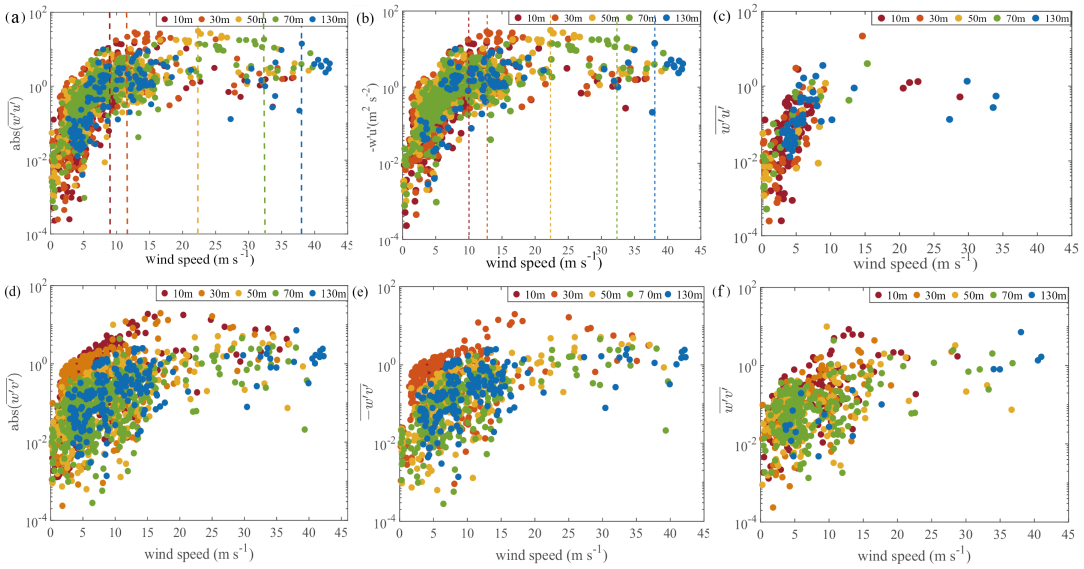

Figure 5 Relationships of turbulent components (abs($\overline{w'u'}$) and abs($\overline{w'v'}$)) as function of u_n from the five levels from the two towers during Typhoon Maria. The overbar indicates time averaging over 10 min. - $\overline{w'u'}$ indicates the negative tangential component fluxes, $\overline{w'u'}$ represents the positive tangential component fluxes, - $\overline{w'v'}$ is the negative radial components flux and $\overline{w'v'}$ is the positive radial components flux. The purple circles are the samples of 10 m, the orange circles are the samples of 30 m, the yellow circles are the samples of 50 m, the

green circles are the samples of 70 m and the blue circles are the samples of 130 m.